

Quasi-homography Warps in Image Stitching

Nan Li, Yifang Xu, and Chao Wang

Abstract—Naturalness of warping is gaining extensive attention in image stitching. Recent warps such as SPHP, AANAP and GSP, use a global similarity to effectively mitigate projective distortion (which enlarges regions), however, they necessarily bring in perspective distortion (which generates inconsistency). In this paper, we propose a quasi-homography warp, which balances perspective distortion against projective distortion in the non-overlapping region, to create natural-looking mosaics. Our approach formulates the warp as a solution of a system of bivariate equations, where perspective distortion and projective distortion are characterized as slope preservation and scale linearization respectively. Our proposed warp only relies on a global homography thus is totally parameter-free. A comprehensive experiment shows that quasi-homography outperforms some state-of-the-art warps in urban scenes, including homography, AutoStitch and SPHP. A user study demonstrates that quasi-homography wins most users’ favor as well, comparing to homography and SPHP.

Index Terms—Image stitching, image warping, projective distortion, perspective distortion.

I. INTRODUCTION

IMAGE stitching plays an important role in many multimedia applications, such as panoramic videos [1]–[3], virtual reality [4]–[6], etc. Basically, it is a process of combining multiple images with overlapping fields of views to produce a wide-view panorama [7], where the first stage is determining a warp for each image to transform it in a common coordinate system, then the warped images are composed [8]–[12] and blended [13]–[15] into a final mosaic. Evaluation of warping includes alignment quality in the overlapping region and naturalness quality in the non-overlapping region.

Early warps focus on improving alignment quality. A global warp such as similarity or projective [16], aims to minimize alignment errors between overlapping pixels by a uniform transformation. Homography is the most frequently used one, because it is the farthest planar transformation where straight lines are preserved in the warped image. However, it usually suffers from projective distortion (which enlarges regions) in the non-overlapping region (see Fig. 1(b)). Some warps address alignment issues due to parallax in the overlapping region, by using multiple local transformations instead of a single global one [17]–[20], or by combining image alignment with seam-cutting approaches [21]–[23].

Recently, some warps such as shape-preserving half-projective (SPHP) warp [24], adaptive as-natural-as-possible (AANAP) warp [25], and warp with global similarity prior (GSP) [26], address naturalness issues in the non-overlapping

N. Li is with the Center for Applied Mathematics, Tianjin University, Tianjin 300072, China. E-mail: nan@tju.edu.cn.

Y. Xu is with the Center for Combinatorics, Nankai University, Tianjin 300071, China. Email: xfy@mail.nankai.edu.cn.

C. Wang is with the Department of Software, Nankai University, Tianjin 300071, China. Email: wangchao@nankai.edu.cn.

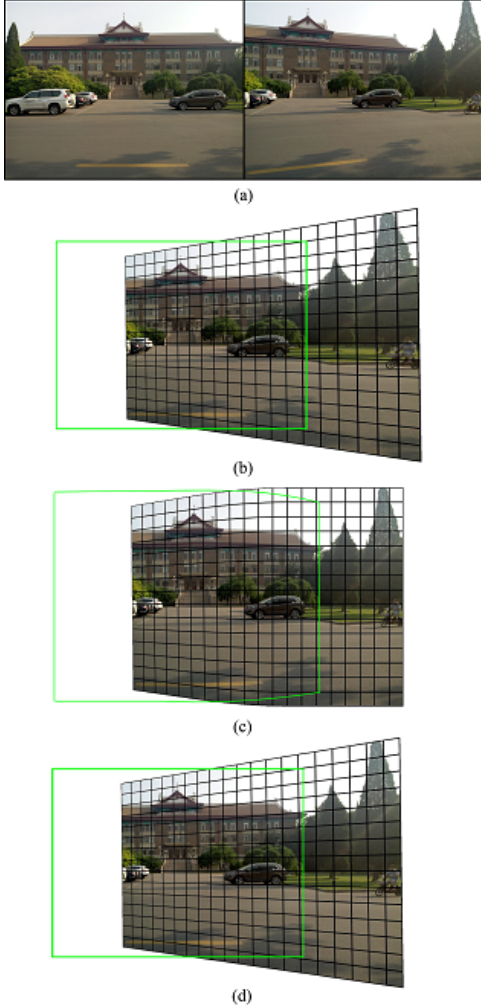


Fig. 1. A distortion comparison among different warps in the non-overlapping region, which uses the same global homography alignment in the overlapping region. (a) Reference and target images. (b) Warped result of homography, which introduces projective distortion in people. (c) Warped result of SPHP, which generates perspective distortion in buildings. (d) Warped result of quasi-homography, that balances projective distortion against perspective distortion.

region by using a global similarity. Though they effectively mitigate projective distortion, they necessarily bring in perspective distortion (which generates inconsistency), because similarity transformations keep original perspectives individually (see Fig. 1(c)). It motivates us to propose a novel warp, that overcomes drawbacks of homography and similarity transformations, to mitigate projective distortion and perspective distortion simultaneously in the non-overlapping region (see Fig. 1(d)).

In this paper, we propose a *quasi-homography* warp, which balances projective distortion against perspective distortion in the non-overlapping region, to create natural-looking mosaics



Fig. 2. A distortion comparison among different warps in the non-overlapping region, which employs the same homography alignment and the same seam-cutting composition [27] in the overlapping region. In final stitching results, we use **blue** rectangles to highlight a comparison of projective distortion, and **red** rectangles to highlight a comparison of perspective distortion.

(see Fig. 2). Our proposed warp only relies on a global homography thus is totally parameter-free. The rest of the paper is organized as follows. Section II describes some of recent related works. Section III provides a detailed derivation of our proposed warp. In particular, Section III-A presents an analysis of homography and SPHP warps, where perspective distortion is addressed by preserving corresponding slopes of horizontal lines and vertical lines, and projective distortion is described in terms of linearizing a scale function. Section III-B reformulates homography as a solution of a system of bivariate equations, where slope preservation and scale linearization are characterized respectively. In Section III-C, we linearize the scale function to a piece-wise C^1 continuous function, and define our quasi-homography warp as a solution of a modified system. Some implementation details (including two-image stitching and multiple-image stitching) and variations (including orthogonal rectification and partition refinement) are proposed in Section IV. Section V presents a comparison experiment and a user study, which demonstrate that our proposed warp not only outperforms some state-of-the-art warps in urban scenes, but also wins most users favor. Finally, conclusions are drawn in Section VI.

II. RELATED WORK

In the following, we review recent works of image warping in aspects of alignment and naturalness respectively. For more fundamental concepts about image stitching, please refer to a comprehensive survey [7] by Szeliski.

A. Warps for Better Alignment

Conventional stitching methods usually use global warps such as affine, similarity and homography, to align images in

the overlapping region [16]. Global warps are robust but often not flexible enough to provide accurate alignment. Gao *et al.* [17] proposed a dual-homography warp to address scenes with two dominant planes by a weighted sum of two homographies. Lin *et al.* [18] proposed a smoothly varying affine warp to replace a global affine transformation with a smoothly affine stitching field, which is more flexible and maintains much of the motion generalization properties of affine or homography. Zaragoza *et al.* [19] proposed an as-projective-as-possible warp in a moving DLT framework, which is able to accurately align images that differ by more than a pure rotation. Lou *et al.* [20] proposed a local alignment method by piecewise planar region matching, which approximates image regions with planes by incorporating piecewise local geometric models.

Other methods combine image alignment with seam-cutting approaches [27]–[30], to find a locally registered area instead of aligning the overlapping region globally. Gao *et al.* [21] proposed a seam-driven stitching framework, which searches a homography with minimal seam costs instead of minimal alignment errors. Zhang and Liu [22] proposed a parallax-tolerant warp, which combines homography and content-preserving warps to locally align images. Lin *et al.* [23] proposed a seam-guided local alignment method, which iteratively improves warping by adaptive feature weighting according to their distances to current seams.

These methods focus on improving alignment quality in the overlapping region, so they sometimes suffer from naturalness issues in the non-overlapping region (see Fig. 2).

B. Warps for Better Naturalness

Many efforts have been devoted to mitigate distortion in the non-overlapping region to create natural-looking mosaics. A pioneering work [31] uses spherical or cylindrical warps to provide multi-perspective results to address this problem, however, it necessarily curves straight lines.

Recently, some methods take the advantage of global similarity (preserve original perspective) to mitigate projective distortion. Chang *et al.* [24] proposed a SPHP warp, which spatially combines a projective and a similarity, where the projective maintains good alignment in the overlapping region while the similarity keeps original perspective in the non-overlapping region. Lin and Pankanti [25] proposed an AANAP warp, which combines a linearized homography and a global similarity with smallest rotation angle to create natural-looking mosaics. Chen *et al.* [26] proposed a GSP warp to stitch multiple images with a global similarity prior in the objective function, which constrains the warp resembles a similarity as a whole.

These methods use a global similarity to effectively mitigate projective distortion in the non-overlapping region, assuming that the original images are most natural to users. However, the assumption is not consistent with human perception in urban scenes, due to the perspective distortion generated by different perspectives between images (see Fig. 2).

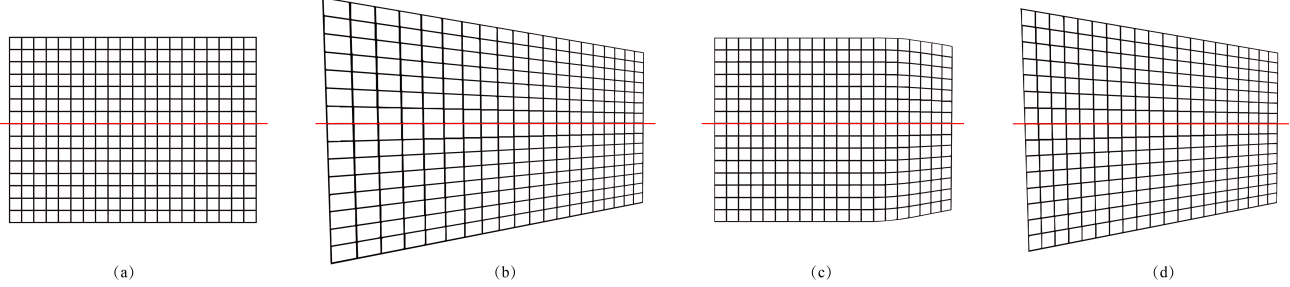


Fig. 3. Perspective distortion v.s. slope preservation. (a) Target image. (b) Warped result of homography. (c) Warped result of SPHP. (d) Our warped result.

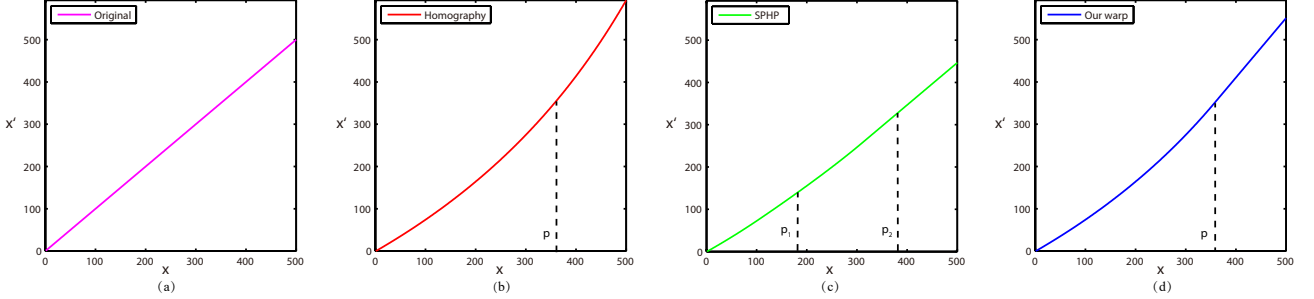


Fig. 4. Projective distortion v.s. scale linearization. It demonstrates scale functions of different warps on a special horizontal line (marked red in Fig. 3).

III. PROPOSED WARPS

In this section, we first present an analysis of homography and SPHP warps, to show their advantages and disadvantages in aspect of perspective distortion or projective distortion (see Fig. 3 and 4), then homography is reformulated as a solution of a system of bivariate equations, where projective distortion is quantified by a nonlinear scale function on a special horizontal line (see Fig. 5(b)), finally quasi-homography is proposed as a solution of a modified system, by linearizing the scale function to a piece-wise \mathcal{C}^1 continuous function (see Fig. 5(c)).

A. Analysis of Homography and SPHP Warps

Let I and I' denote the *target image* and the *reference image* respectively. A warp \mathcal{H} is a planar transformation [16], which relates pixel coordinates $(x, y) \in I$ to $(x', y') \in I'$, where

$$\begin{cases} x' = f(x, y) \\ y' = g(x, y) \end{cases}. \quad (1)$$

We say a warp is *line-preserving*, if any straight line in the target image is transformed into a straight line in the warped result. If a line-preserving warp aligns the target image to the reference image, then the perspective of the warped result is consistent with the perspective of the reference image. Given a line-preserving warp \mathcal{H} as (1) and a line with slope k crossing $(x, y) \in I$, then it is corresponding to a line with slope $\text{slope}(x, y, k)$ crossing $(x', y') \in I'$, where

$$\text{slope}(x, y, k) = \frac{g(x + z, y + kz) - g(x, y)}{f(x + z, y + kz) - f(x, y)} \quad (\forall z \in \mathbb{R}) \quad (2)$$

$$= \lim_{z \rightarrow 0} \frac{g(x + z, y + kz) - g(x, y)}{f(x + z, y + kz) - f(x, y)} \quad (3)$$

$$= \frac{g_x(x, y) + kg_y(x, y)}{f_x(x, y) + kf_y(x, y)}, \quad (4)$$

and f_x, f_y, g_x, g_y denote partial derivatives of f and g . In fact, (2) is a sufficient and necessary condition of a line-preserving warp. In order to characterize perspective distortion, we draw a grid-to-grid map of lines with slopes

$$\text{slope}(x, y, 0) = \frac{g_x(x, y)}{f_x(x, y)}, \quad (5)$$

$$\text{slope}(x, y, \infty) = \frac{g_y(x, y)}{f_y(x, y)}, \quad (6)$$

which are corresponding to horizontal lines and vertical lines in the target image. Consequently, any point $(x, y) \in I$ can be regarded as the intersection point of a horizontal line and a vertical line, which is corresponding to a point $(x', y') \in I'$ as the intersection point of lines with slopes (5,6) (see Fig. 3).

It is easy to check that a homography warp \mathcal{H}_0

$$f_0(x, y) = \frac{h_1x + h_2y + h_3}{h_7x + h_8y + 1}, \quad (7)$$

$$g_0(x, y) = \frac{h_4x + h_5y + h_6}{h_7x + h_8y + 1}, \quad (8)$$

satisfies condition (2), therefore homography is line-preserving (see Fig. 3(b)). However, SPHP is not line-preserving, because projective's perspective in the overlapping region is inconsistent with similarity's perspective in the non-overlapping region (see Fig. 3(c)).

In horizontal image stitching, there always exists a special horizontal line $y = y_*$, that preserves horizontal under a line-preserving warp, where y_* is determined by solving

$$\text{slope}(x, y_*, 0) = \frac{g_x(x, y_*)}{f_x(x, y_*)} = 0. \quad (9)$$

In fact, $f(x, y_*)$ is a scale function on the special horizontal line, which quantifies projective distortion in horizontal image

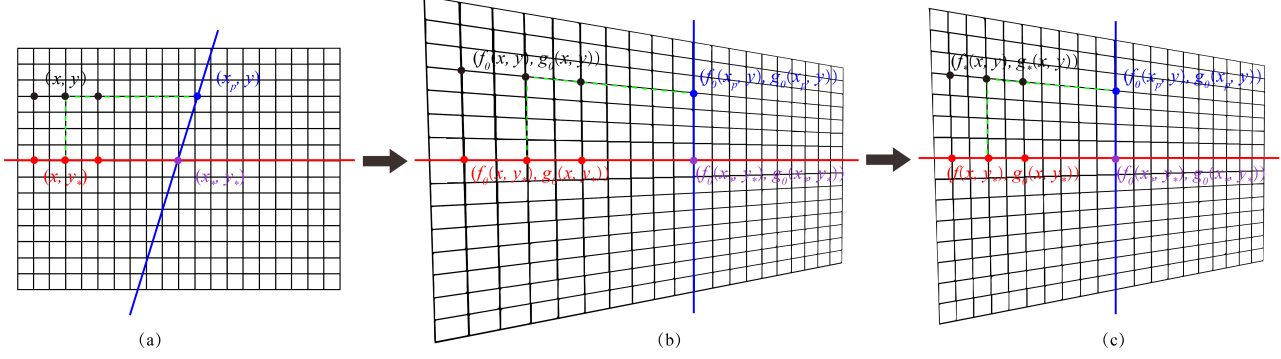


Fig. 5. Quasi-homography v.s. homography. (a) Target image. (b) Reformulation of homography. (c) Derivation of quasi-homography. In the non-overlapping region, quasi-homography not only preserves corresponding slopes of grids as homography, but also possesses a linear scale function on the special horizontal line as similarity.

stitching. In order to characterize the function more explicitly, we draw a map $x \mapsto f(x, y_*)$ (see Fig. 4).

Given a homography warp \mathcal{H}_0 as (7,8), we can obtain

$$y_* = \frac{h_6h_7 - h_4}{h_4h_8 - h_5h_7}, \quad (10)$$

$$f_0(x, y_*) = \frac{(h_4h_8 - h_5h_7)(h_1x + h_3) + (h_6h_7 - h_4)h_2}{(h_4h_8 - h_5h_7)h_7x + (h_6h_8 - h_5)h_7}. \quad (11)$$

Homography necessarily generates projective distortion, because the derivative $f'_0(x, y_*)$ constantly increases in the non-overlapping region (see Fig. 4(b)). However, SPHP possesses a piece-wise \mathcal{C}^1 continuous scale function, which is linear in the non-overlapping region (see Fig. 4(c)). This difference leads to less projective distortion of SPHP than homography.

B. Reformulation of Homography Warps

Suppose I and I' are well-aligned by a global homography \mathcal{H}_0 as (7,8) in the overlapping region, our goal is to propose a warp \mathcal{H}_* that combines the advantages of homography (line-preserving) and similarity (a linear scale function) in the non-overlapping region. In the following, we give a reformulation of homography, that characterizes slope preservation and scale linearization respectively.

First, we define $x = x_p$ as the preimage of the border of the overlapping region and the non-overlapping region (marked in blue in Fig. 5(a)), which satisfies

$$f(x_p, y) = p, \quad (12)$$

where $p = 0$ if assigning the left image as the target image I , otherwise p equals to the width of the reference image I' .

For a homography \mathcal{H}_0 , the preimage

$$x_p = \frac{(ph_8 - h_2)y - h_3 + p}{h_1 - ph_7}. \quad (13)$$

Then, in order to benefit from the analysis of homography and SPHP, we reformulate homography as a solution of

$$\frac{g(x, y) - g_0(x_p, y)}{f(x, y) - f_0(x_p, y)} = \text{slope}(x, y, 0), \quad (14)$$

$$\frac{g(x, y) - g_0(x, y_*)}{f(x, y) - f_0(x, y_*)} = \text{slope}(x, y, \infty), \quad (15)$$

where (x_p, y) and (x, y_*) are projections of (x, y) onto $x = x_p$ and $y = y_*$ respectively (see Fig. 5(a)), and

$$\text{slope}(x, y, 0) = \frac{(h_4h_8 - h_5h_7)y - h_6h_7 + h_4}{(h_1h_8 - h_2h_7)y - h_3h_7 + h_1}, \quad (16)$$

$$\text{slope}(x, y, \infty) = \frac{(h_4h_8 - h_5h_7)x + h_6h_8 - h_5}{(h_1h_8 - h_2h_7)x + h_3h_8 - h_2}, \quad (17)$$

which are independent of x and y respectively.

It is easy to check that, if we regard $f(x, y)$ and $g(x, y)$ as unknowns, then \mathcal{H}_0 as (7,8) is the unique solution of (14,15) satisfying (10,13,16,17). Comparing to the formulation (7,8), our reformulation characterizes perspective distortion as slope preservation ($\text{slope}(x, y, 0)$ and $\text{slope}(x, y, \infty)$) and projective distortion as scale linearization ($f_0(x, y_*)$) respectively. In fact, $\text{slope}(x, y, 0)$ and $\text{slope}(x, y, \infty)$ constrain shapes of the grid, while $f_0(x, y_*)$ determines its density (see Fig. 5(b)).

C. Quasi-homography Warps

Our reformulation of homography and our analysis of SPHP motivate us to modify $f_0(x, y_*)$ to a piece-wise \mathcal{C}^1 continuous function, which is linear in the non-overlapping region.

First, the special horizontal line $y = y_*$ (13) intersects the preimage $x = x_p$ (10) at

$$x_* = \frac{(h_5h_7 - h_6h_7h_8)p + h_2(h_6h_7 - h_4)}{(h_4h_8 - h_5h_7)(ph_7 - h_1)} + \frac{h_3}{ph_7 - h_1}. \quad (18)$$

Then, the truncation of Taylor's expansion of $f_0(x, y_*)$,

$$f_*(x, y_*) = p + \frac{(h_1h_8 - h_2h_7)y_* + (h_1 - h_3h_7)}{(h_7x_* + h_8y_* + 1)^2}(x - x_*), \quad (19)$$

is linear in the non-overlapping region and is \mathcal{C}^1 connected to $f_0(x, y_*)$ in the overlapping region. Let \mathcal{O} denote the overlapping region, we modify the scale function to

$$f_*(x, y_*) = \begin{cases} f_0(x, y_*), & \text{if } (x, y_*) \in \mathcal{O}, \\ f_*(x, y_*), & \text{otherwise,} \end{cases} \quad (20)$$

which is piece-wise \mathcal{C}^1 continuous. If we regard $f(x, y)$ and

$g(x, y)$ as unknowns, then the system of bivariate equations

$$\frac{g(x, y) - g_0(x_p, y)}{f(x, y) - f_0(x_p, y)} = \text{slope}(x, y, 0), \quad (21)$$

$$\frac{g(x, y) - g_0(x, y_*)}{f(x, y) - f_*(x, y_*)} = \text{slope}(x, y, \infty), \quad (22)$$

satisfying (10,13,16,17,20) possess a unique solution \mathcal{H}_\dagger

$$f_\dagger(x, y) = \begin{cases} f_0(x, y), & \text{if } (x, y_*) \in \mathcal{O}, \\ f_*(x, y), & \text{otherwise,} \end{cases} \quad (23)$$

$$g_\dagger(x, y) = \begin{cases} g_0(x, y), & \text{if } (x, y_*) \in \mathcal{O}, \\ g_*(x, y), & \text{otherwise,} \end{cases} \quad (24)$$

where

$$f_*(x, y) = \frac{w_1 x^2 y + w_2 x^2 + w_3 x y + w_4 x + w_5 y + w_6}{h_7 x + h_8 y + 1}, \quad (25)$$

$$g_*(x, y) = \frac{w_7 x^2 y + w_8 x^2 + w_9 x y + w_{10} x + w_{11} y + w_{12}}{h_7 x + h_8 y + 1}, \quad (26)$$

define a warp \mathcal{H}_* in the non-overlapping region and w_1, \dots, w_{12} are polynomials in p, h_1, \dots, h_8 .

In fact, the warp \mathcal{H}_\dagger just crowds the grid of homography in the horizontal direction but without varying its shape (see Fig. 5(c)). In this sense, we call \mathcal{H}_\dagger a *quasi-homography* warp corresponding to a homography warp \mathcal{H}_0 . A quasi-homography \mathcal{H}_\dagger maintains good alignment in the overlapping region as \mathcal{H}_0 while mitigates perspective distortion and projective distortion simultaneously as \mathcal{H}_* in the non-overlapping region.

If a homography warp \mathcal{H}_0 (7,8) is an injection in the image domain, then its corresponding quasi-homography warp \mathcal{H}_\dagger is also an injection. Therefore, given $(x', y') \in I'$, then $(x, y) \in I$ is determined by an inverse map

$$\mathcal{H}_\dagger^{-1} = \begin{cases} \mathcal{H}_0^{-1}, & \text{if } (x, y_*) \in \mathcal{O}, \\ \mathcal{H}_*^{-1}, & \text{otherwise,} \end{cases} \quad (27)$$

where \mathcal{H}_*^{-1}

$$x = \text{RootOf}(m_1 x^2 + m_2 x + m_3), \quad (28)$$

$$y = -\frac{h_4 x' - h_6 h_7 x' - h_1 y' + h_3 h_7 y' - h_3 h_4 + h_1 h_6}{h_4 h_8 x' - h_5 h_7 x' - h_1 h_8 y' + h_2 h_7 y' - h_2 h_4 + h_1 h_5}, \quad (29)$$

and m_1, \dots, m_3 are polynomials in $x', y', p, h_1, \dots, h_8$.

IV. IMPLEMENTATION

In this section, we first present more implementation details of our quasi-homography in two-image stitching and multiple-image stitching, and then we propose two variations including orthogonal rectification and partition refinement.

A. Two-image Stitching

Given two images captured from a camera rotated vertically, if a homography \mathcal{H}_0 is estimated, then a quasi-homography \mathcal{H}_\dagger can be calculated, which smoothly extrapolates \mathcal{H}_0 in the overlapping region to \mathcal{H}_* in the non-overlapping region. A brief algorithm is given in Algorithm 1.

Algorithm 1 Image stitching using quasi-homography.

Input: two images taken from a camera rotated vertically.

Output: one horizontally stitched image.

- 1) Use SIFT [32] to extract and match features;
- 2) Use RANSAC [33] to estimate a global homography \mathcal{H}_0 ;
- 3) Calculate a quasi-homography warp:
 - a) Calculate a forward map \mathcal{H}_\dagger (23,24) to get the canvas;
 - b) Calculate a backward map \mathcal{H}_\dagger^{-1} (27) to fill the canvas by bilinear interpolations;
- 4) Use seam-cutting [27] to blend the overlapping region.

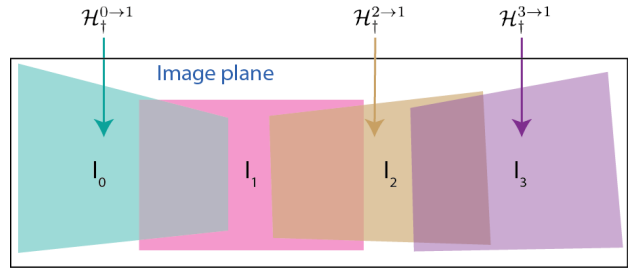


Fig. 6. Stitching multiple images. Coordinates of other images are transformed to the coordinate system of the reference image I_1 .

B. Multiple-image Stitching

Given a sequence of multiple images, which are captured from a camera rotated vertically, our warping method consists of three stages. In the first stage, we determine a reference image as the standard perspective. Then, we estimate a homography for every two images with overlapping fields of views, and calculate its corresponding quasi-homography. Finally, we concatenate all target images in the image plane of the reference image.

Fig. 6 illustrates the concatenation procedure of stitching four images. First, we set I_1 as the reference image, so perspectives of other target images should agree with its perspective. Then, we calculate quasi-homography warps $\mathcal{H}_\dagger^{0 \rightarrow 1}$, $\mathcal{H}_\dagger^{2 \rightarrow 1}$ and $\mathcal{H}_\dagger^{3 \rightarrow 2}$. Finally, we concatenate I_3 to I_1 by

$$\mathcal{H}_\dagger^{3 \rightarrow 1} = \mathcal{H}_\dagger^{2 \rightarrow 1} \circ \mathcal{H}_0^{3 \rightarrow 2}. \quad (30)$$

For stitching more images, we obtain the concatenation maps recursively.

C. Orthogonal Rectification

In urban scenes, users accustom to take pictures by rotating cameras vertically, hence any vertical line in the target image is expected to transform to a vertical line in the warped result. However, it will inevitably sacrifice alignment quality in the overlapping region.

In order to achieve orthogonal rectification, we incorporate an extra constraint in homography estimation, which constrains the external vertical boundary of the target image preserves vertical in the warped result. Then, it should satisfy

$$f(p, 0) = f(p, h), \quad (31)$$

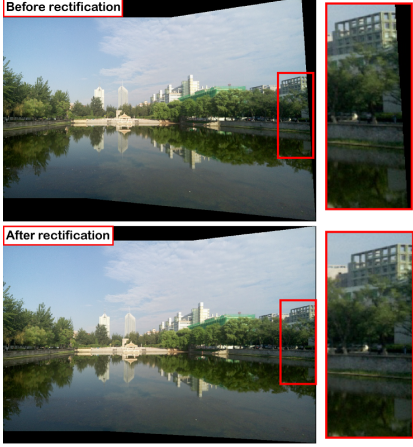


Fig. 7. An example of orthogonal rectification.

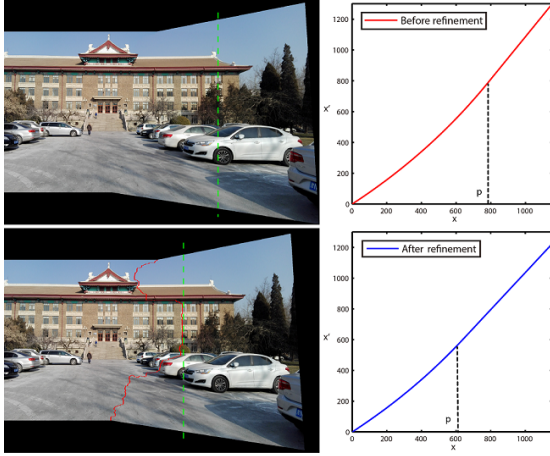


Fig. 8. An example of partition refinement.

where h is the height of the target image and $p = 0$ if assigning the left image as target, otherwise p equals to the width of the target image. For a homography warp \mathcal{H}_0 as (7,8), we obtain

$$h_8 = \frac{h_2(h_7p + h_9)}{h_1p + h_3}. \quad (32)$$

Then, a global homography is estimated by solving

$$\min \sum_{i=1}^N \|\mathbf{a}_i \mathbf{h}\|^2 \text{ s.t. } \|\mathbf{h}\| = 1, h_8 = \frac{h_2(h_7p + h_9)}{h_1p + h_3}. \quad (33)$$

Since quasi-homography just crowds the grid of homography in the horizontal direction but without varying its shape, so the external vertical boundary still preserves vertical (see Fig. 7).

D. Partition Refinement

In (12), we simply set the partition line x_p as the border of the overlapping region and the non-overlapping region, which directly determines the linear scale function (19). In fact, the scale ratio

$$\rho = \frac{(h_1h_8 - h_2h_7)y_* + (h_1 - h_3h_7)}{(h_7x_* + h_8y_* + 1)^2} \quad (34)$$

is more precise when (x_*, y_*) is more locally aligned, thus we modify the partition line x_p as the external border of the seam for further refinement (see Fig. 8).

V. EXPERIMENTS

We experimented our proposed method on a range of images captured from rear and front cameras in urban scenes. In our experiments, we use SIFT [32] to extract and match features, RANSAC [33] to estimate a global homography, and seam-cutting [27] to blend the overlapping region. Codes are implemented in OpenCV 2.4.9 and generally take 1s-2s on a desktop PC with Intel i5 3.0GHz CPU and 8GB memory to stitch two images with 800×600 resolution by Algorithm IV-A, where the calculation of quasi-homography only takes 0.1s (including forward map and backward map).

A. Comparisons to State-of-the-art Warps

We compared our quasi-homography warp to state-of-the-art warps in urban scenes, including homography, SPHP and AutoStitch. In order to highlight comparisons on naturalness quality in the non-overlapping region, for homography, SPHP and quasi-homography, we use the same homography alignment and the same seam-cutting composition in the overlapping region. More results and original input images are available in the supplementary material.

Fig. 9 illustrates an example in selfie-stitching. Homography provides a line-preserving stitching result but generates projective distortion in buildings and trees (highlighted in blue rectangles). SPHP mitigates projective distortion significantly but brings in apparent perspective distortion in the top of buildings (highlighted in red rectangles). Quasi-homography creates a more natural-looking stitching result in both aspects of projective distortion and perspective distortion.

Fig. 10 illustrates an example in multiple-image stitching, where stitching results are cropped for the sake of layout. Homography enlarges trees on the right (highlighted in blue rectangles) but preserves all straight lines. SPHP curves buildings and grounds (highlighted in red rectangles) but without enlarging the region of trees. AutoStitch produces a fisheye-like mosaic due to spherical warps. Quasi-homography balances projective distortion against perspective distortion by preserving horizontal lines and vertical lines, simultaneously possessing a piece-wise \mathcal{C}^1 continuous scale function.

B. User Study

In order to investigate whether quasi-homography is preferred by users in urban scenes, we conduct a user study to compare our result to homography and SPHP. We invite 17 participants to rank 20 unannotated groups of stitching results, including 5 groups from front camera and 15 groups from rear camera. In each group, we use the same homography alignment and the same seam-cutting composition, and all parameters are set to produce the optimal results. In our study, each participant ranks three unannotated stitching results in each group, and a score is counted by assigning weights 4, 2 and 1 to Rank 1, Rank 2 and Rank 3.

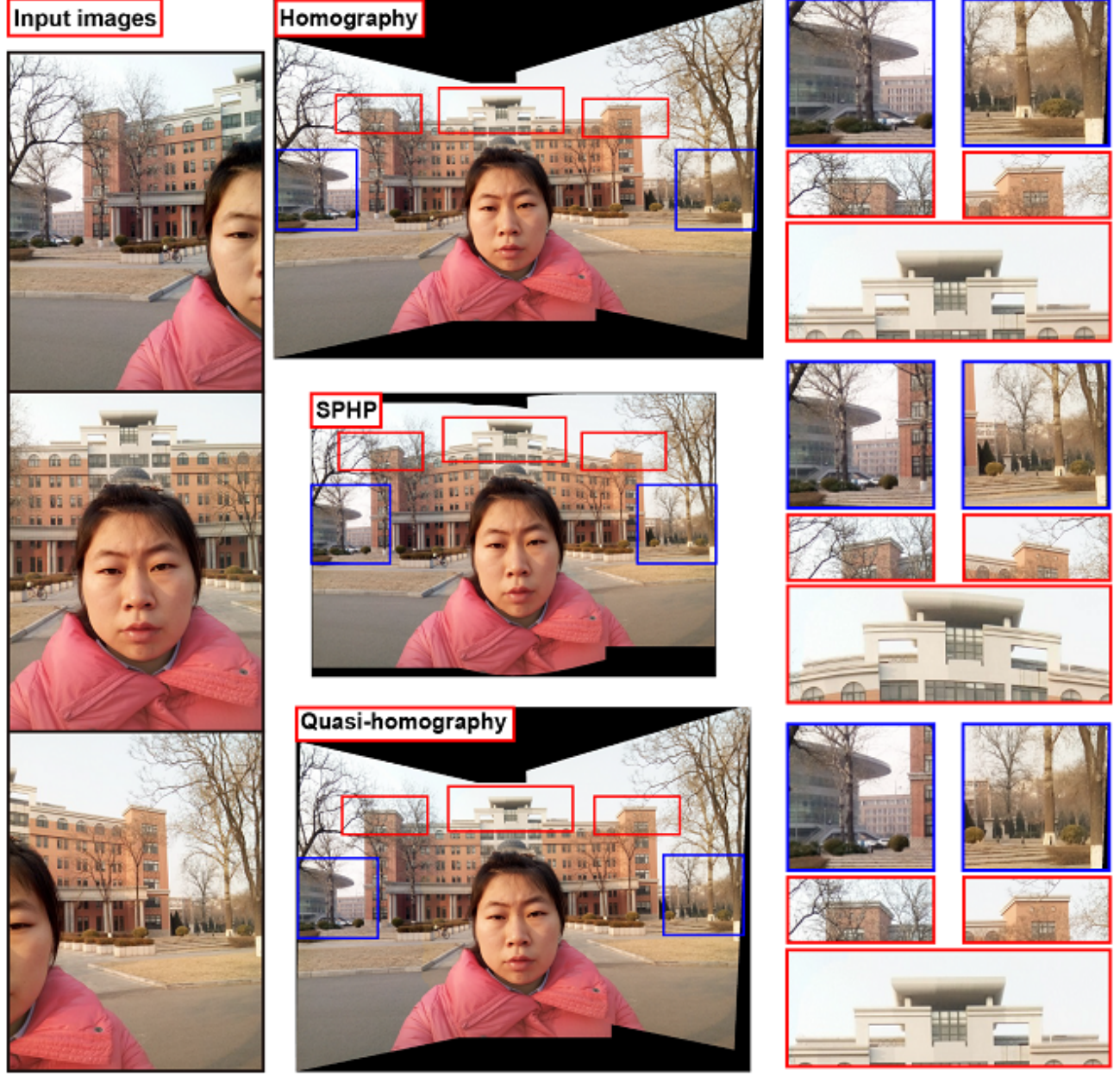


Fig. 9. A distortion comparison among different warps in the non-overlapping region in selfie-stitching, which employs the same homography alignment and the same seam-cutting composition [27] in the overlapping region. In final stitching results, we use blue rectangles to highlight a comparison of projective distortion, and red rectangles to highlight a comparison of perspective distortion.

Table I shows a summary of rank vote and total score for three warps, and the histogram of the score is shown in Fig. 11 in three aspects. This user study demonstrates that stitching results of quasi-homography win most users' favor in urban scenes.

VI. CONCLUSION

In this paper, we propose a quasi-homography warp, which balances perspective distortion against projective distortion in the non-overlapping region, to create natural-looking mosaics. Experiments show that quasi-homography outperforms some state-of-the-art warps in urban scenes, including homography, AutoStitch and SPHP. A user study demonstrates that stitching

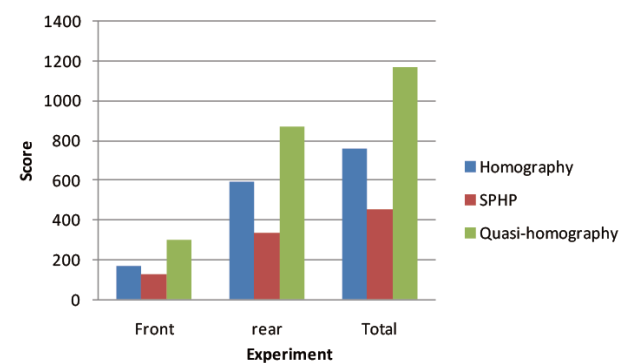


Fig. 11. Score of compared methods in front and rear camera setting.



Fig. 10. A comparison of different warps in stitching four images of teaching building example.

TABLE I
THE COMPARISON RESULTS FOR THREE METHODS.

Methods	Results			
	Rank 1	Rank 2	Rank 3	Total score
Homography	69	210	61	757
SPHP [24]	19	56	265	453
Quasi-homography	252	74	14	1170

results of quasi-homography win most users' favor as well, comparing to homography and SPHP. It should be noted that, though quasi-homography preserves horizontal lines and vertical lines, it may curve some diagonal lines in the stitching result. Fortunately, users accustom to take pictures of orthogonal compositions in urban scenes. Future works may include generalizing quasi-homography warps in the spatially-varying warping framework to improve alignment quality.

REFERENCES

- [1] S. Tzavidas and A. K. Katsaggelos, "A multicamera setup for generating stereo panoramic video," *IEEE Transactions on Multimedia*, vol. 7, no. 5, pp. 880–890, 2005.
- [2] X. Sun, J. Foote, D. Kimber, and B. S. Manjunath, "Region of interest extraction and virtual camera control based on panoramic video capturing," *IEEE Transactions on Multimedia*, vol. 7, no. 5, pp. 981–990, 2005.
- [3] V. R. Gaddam, M. Riegler, R. Eg, and P. Halvorsen, "Tiling in interactive panoramic video: Approaches and evaluation," *IEEE Transactions on Multimedia*, vol. 18, no. 9, pp. 1–1, 2016.
- [4] H. Y. Shum, K. T. Ng, and S. C. Chan, "A virtual reality system using the concentric mosaic: construction, rendering, and data compression," *IEEE Transactions on Multimedia*, vol. 7, no. 1, pp. 85–95, 2005.
- [5] W. K. Tang, T. T. Wong, and P. A. Heng, "A system for real-time panorama generation and display in tele-immersive applications," *IEEE Transactions on Multimedia*, vol. 7, no. 2, pp. 280–292, 2005.
- [6] Q. Zhao, L. Wan, W. Feng, and J. Zhang, "Cube2video: Navigate between cubic panoramas in real-time," *IEEE Transactions on Multimedia*, vol. 15, no. 8, pp. 1745–1754, 2013.
- [7] R. Szeliski, "Image alignment and stitching: A tutorial," *Found. Trends Comput. Graph. Vis.*, vol. 2, no. 1, pp. 1–104, 2006.
- [8] S. Peleg, "Elimination of seams from photomosaics," *Comput. Graph. Image Process.*, vol. 16, no. 1, pp. 90–94, 1981.
- [9] M.-L. Duplaquet, "Building large image mosaics with invisible seam lines," in *Proc. SPIE Visual Information Processing VII*, 1998, pp. 369–377.
- [10] J. Davis, "Mosaics of scenes with moving objects," in *Proc. IEEE Conf. Comput. Vis. Pattern Recog.*, June. 1998, pp. 354–360.
- [11] A. A. Efros and W. T. Freeman, "Image quilting for texture synthesis and transfer," in *Proc. ACM SIGGRAPH*, 2001, pp. 341–346.
- [12] A. Mills and G. Dudek, "Image stitching with dynamic elements," *Image Vis. Comput.*, vol. 27, no. 10, pp. 1593–1602, 2009.
- [13] P. J. Burt and E. H. Adelson, "A multiresolution spline with application to image mosaics," *ACM Trans. Graphics*, vol. 2, no. 4, pp. 217–236, 1983.
- [14] P. Pérez, M. Gangnet, and A. Blake, "Poisson image editing," *ACM Trans. Graphics*, vol. 22, no. 3, pp. 313–318, 2003.
- [15] A. Levin, A. Zomet, S. Peleg, and Y. Weiss, "Seamless image stitching in the gradient domain," in *Proc. Eur. Conf. Comput. Vis.*, May 2004, pp. 377–389.
- [16] R. Hartley and A. Zisserman, *Multiple view geometry in computer vision*. Cambridge univ. press, 2003.
- [17] J. Gao, S. J. Kim, and M. S. Brown, "Constructing image panoramas using dual-homography warping," in *Proc. IEEE Conf. Comput. Vis. Pattern Recog.*, Jun. 2011, pp. 49–56.
- [18] W.-Y. Lin, S. Liu, Y. Matsushita, T.-T. Ng, and L.-F. Cheong, "Smoothly varying affine stitching," in *Proc. IEEE Conf. Comput. Vis. Pattern Recog.*, Jun. 2011, pp. 345–352.
- [19] J. Zaragoza, T.-J. Chin, M. S. Brown, and D. Suter, "As-projective-as-possible image stitching with moving DLT," in *Proc. IEEE Conf. Comput. Vis. Pattern Recog.*, Jun. 2013, pp. 2339–2346.
- [20] Z. Lou and T. Gevers, "Image alignment by piecewise planar region matching," *IEEE Transactions on Multimedia*, vol. 16, no. 7, pp. 2052–2061, 2014.
- [21] J. Gao, Y. Li, T.-J. Chin, and M. S. Brown, "Seam-driven image stitching," *Eurographics*, pp. 45–48, 2013.
- [22] F. Zhang and F. Liu, "Parallax-tolerant image stitching," in *Proc. IEEE Conf. Comput. Vis. Pattern Recog.*, May. 2014, pp. 3262–3269.
- [23] K. Lin, N. Jiang, L.-F. Cheong, M. Do, and J. Lu, "Seagull: Seam-guided local alignment for parallax-tolerant image stitching," in *Proc. Eur. Conf. Comput. Vis.*, Oct. 2016.
- [24] C.-H. Chang, Y. Sato, and Y.-Y. Chuang, "Shape-preserving half-projective warps for image stitching," in *Proc. IEEE Conf. Comput. Vis. Pattern Recog.*, May 2014, pp. 3254–3261.
- [25] C.-C. Lin, S. U. Pankanti, K. N. Ramamurthy, and A. Y. Aravkin, "Adaptive as-natural-as-possible image stitching," in *Proc. IEEE Conf. Comput. Vis. Pattern Recog.*, Jun. 2015, pp. 1155–1163.
- [26] N. I. S. with the Global Similarity Prior, "Yu-sheng chen and yung-yu chuang," in *Proc. Eur. Conf. Comput. Vis.*, Oct. 2016, pp. 186–201.
- [27] Y. Boykov, O. Veksler, and R. Zabih, "Fast approximate energy minimization via graph cuts," *IEEE Trans. Pattern Anal. Mach. Intell.*, vol. 23, no. 11, pp. 1222–1239, Nov. 2001.
- [28] A. Agarwala, M. Dontcheva, M. Agrawala, S. Drucker, A. Colburn, B. Curless, D. Salesin, and M. Cohen, "Interactive digital photomontage," *ACM Trans. Graphics*, vol. 23, no. 3, pp. 294–302, 2004.
- [29] V. Kwatra, A. Schödl, I. Essa, G. Turk, and A. Bobick, "Graphcut textures: image and video synthesis using graph cuts," *ACM Trans. Graphics*, vol. 22, no. 3, pp. 277–286, 2003.
- [30] A. Eden, M. Uyttendaele, and R. Szeliski, "Seamless image stitching of scenes with large motions and exposure differences," in *Proc. IEEE Conf. Comput. Vis. Pattern Recog.*, vol. 2, Jun. 2006, pp. 2498–2505.
- [31] M. Brown and D. G. Lowe, "Automatic panoramic image stitching using invariant features," *Int. J. Comput. Vis.*, vol. 74, no. 1, pp. 59–73, 2007.
- [32] D. G. Lowe, "Distinctive image features from scale-invariant keypoints," *Int. J. Comput. Vis.*, vol. 60, no. 2, pp. 91–110, 2004.
- [33] M. A. Fischler and R. C. Bolles, "Random sample consensus: a paradigm for model fitting with applications to image analysis and automated cartography," *Commun. ACM*, vol. 24, no. 6, pp. 381–395, 1981.